Characterization of Optical Systems for Radial Metrology

Donald R. Matthys
Physics Department
Marquette University
Milwaukee, Wisconsin 53233

John A. Gilbert
Department of Mechanical and Aerospace Engineering
University of Alabama in Huntsville
Huntsville, Alabama 35899

Sara B. Fair
Consortium for Holography, Applied Mechanics, and Photonics
University of Alabama in Huntsville
Huntsville, Alabama 35899

ABSTRACT

This paper discusses the optical characteristics of a panoramic annular lens (PAL) and develops some of the parametric equations required to design and characterize optical systems for visual inspection and measurement.

1 INTRODUCTION

Radial metrology[1] is the process of making optical inspections and measurements, typically within cavities, using panoramic systems. Although a number of papers have been written that describe how to accomplish such tasks, the analyses relied on complex ray traces and customized computational software.[2] Without a precise knowledge of the underlying details, potential users have had difficulty applying the methods. To make matters worse, many different coordinate systems were used during the development of radial metrology; nomenclature and definitions were often inconsistent from paper to paper.

The objective of this paper is to introduce standard jargon and notation for radial metrology. The optical characteristics of a panoramic annular lens (PAL) are discussed, and some of the parametric equations required to design and characterize optical systems for visual inspection, contour measurement, phase mapping, and stereoscopic imaging are described.

2 THE PANORAMIC ANNULAR LENS (PAL)

The PAL works by a complex combination of reflection and refraction. It is a single element lens composed of three spherical surfaces, two convex and one concave, and one flat surface. Non-adjacent concave and convex surfaces are mirrored, while the flat and the remaining convex surface are not. As illustrated in Fig. 1, the surfaces are uniquely designed to focus and translate the incoming light (from, *e.g.*, points A and B) in much the same way as a series of lenses and mirrors. They form an internal virtual image (A′ and B′) that can be transferred by a standard lens to a CCD camera to form a real image (A′′ and B′′). The annular image contains the images of the objects that surround the PAL.

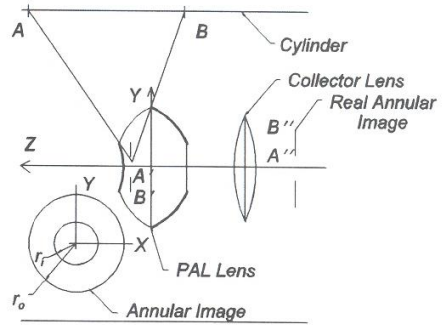

***Figure 1**. An annular image is captured by a panoramic annular lens (PAL).*

In most cases, a longitudinal axis, Z, is chosen to coincide with the optical axis of the lens. A right-handed Cartesian coordinate system is established at the physical center of the PAL where the diameter is the largest. A cylindrical coordinate system can also be introduced with θ measured counterclockwise from the X-axis in the X,Y plane. Assuming that points A and B are located at the edges of the field of view on a cylinder surrounding the lens, all points on the inner wall contained in the plane defined by z = A are imaged around the inner radius, r_i, of the image annulus. Similarly, points on the wall in the plane z = B are imaged around the outer radius, r_o.

In addition to imaging its surroundings, a PAL can be used to illuminate them. Figure 2, for example, shows a 38 mm (1.5 in.) diameter PAL with its optical axis aligned with the longitudinal axis of a pipe having an inner radius equal to R. The characteristics of the lens were determined by combining physical measurements with a ray trace. The entrance pupil center of the PAL is offset a distance of z_e =

6.74 mm (0.26 in.) toward the front of the lens, and y_e = 1.34 mm (0.05 in.) from the optical axis (for object points contained in the Y,Z plane). The angular field of view measured from this point is 45.4° covering the range -18.8° ≤ φ_i ≤ 26.6°, where φ_i is the field angle. By convention, positive field angles are measured toward the front of the lens.

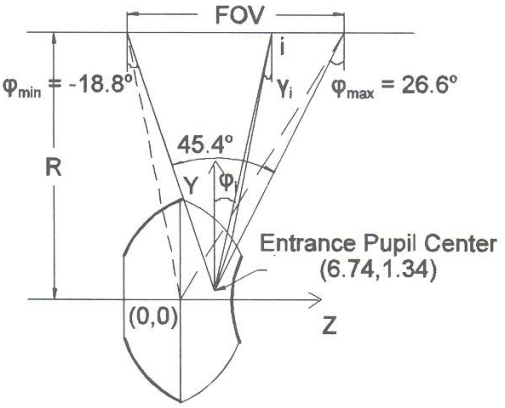

***Figure 2**. Optical characteristics of an illuminating lens.*

The linear distance that can be illuminated or imaged by the lens is defined in Fig. 2 as the field of view (FOV). For the 38 mm (1.5 in.) diameter PAL,

$$FOV = (R - y_e)(\tan 26.6° + \tan 18.8°) \quad . \qquad (1)$$

Not all the rays exiting or entering the lens actually pass through the entrance pupil center, so a linear regression was performed on ray trace data to establish a parametric equation describing the direction of propagation of the illuminating wavefront, given by the angle γ_i, in terms of the field angle, φ_i.[3] For a plane wavefront entering the flat surface of the PAL,

$$\gamma_i = 1.00417\ \varphi_i - 0.2978 \qquad (2)$$

where both angles are measured in degrees. Over the FOV, the propagation directions determined from this equation agree to within ± 2% error with those obtained from the ray trace.

The 38 mm (1.5 in.) diameter PAL has been characterized in terms of spherical aberration and coma, distortion, image plane curvature, and the modulation transfer function.[4] In general, the acceptance angle varies with the field angle; the amount of spherical aberration is proportional to the acceptance angle. The magnification varies quadradically and image plane curvature is cubic.

From an experimental mechanics standpoint, the resolution of the PAL varies from the forward viewing edge to the back viewing edge with an angular resolution of approximately 6 millirads. Even though the PAL is not strictly afocal, objects appear to be in focus from the lens surface to infinity. The transmittance varies less than five percent over the visible light range; however, since the PAL is both refractive and reflective, it does not possess the same performance for all wavelengths.

3 MAPPING CHARACTERISTICS

In radial metrology, the aspect ratio of an area is defined as height divided by width.[5] In real (or object) space, height is measured as the longitudinal distance relative to the optical axis of a lens; width corresponds to the circumferential distance measured around the optical axis. In image space, height is measured as a radial distance relative to the center of an image; width corresponds to a circumferential distance measured around the image center.

When a conventional lens is used to image the inside wall of a cylinder whose inside surface is composed of a uniform grid of squares, the structure is mapped into the image plane as a series of evenly spaced concentric rings representing equally spaced lines drawn around the circumference of the cylinder. Radial lines represent the longitudinal lines drawn along the length of the cylinder at constant circumferential positions. Figure 3(a) illustrates that, in the case of the conventional lens, square elements having a real space aspect ratio of unity are mapped to an image comprised of segments which have different image plane aspect ratios. The PAL maps the same uniform grid of squares into the constant aspect ratio polar map illustrated in Figure 3(b). This unique property results in a higher information density thereby facilitating cavity inspection and measurement.[6]

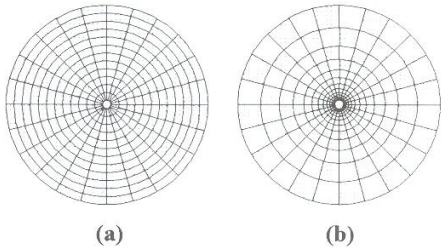

***Figure 3**. A square grid wrapped around the inside wall of a cylinder becomes: a conventional polar map (a) when recorded with a conventional lens, and a constant aspect ratio polar map (b) when recorded with a PAL.*

4 FIELD ANGLES IN A DUAL PAL SYSTEM

Some panoramic measurements are made by combining two collinear panoramic annular lenses (PALs). Figure 4, for example, demonstrates how the object beam can be produced in an interferometric recording system. In this example, the two PALs are located within a section of cylindrical pipe and spaced a distance dz apart. When a coherent light source is used and a reference beam added, interference occurs over the region of interest (ROI) where the beams overlap.

In Fig. 4, a local coordinate system (η,ξ) is introduced at the entrance pupil center of the illuminating PAL from which the

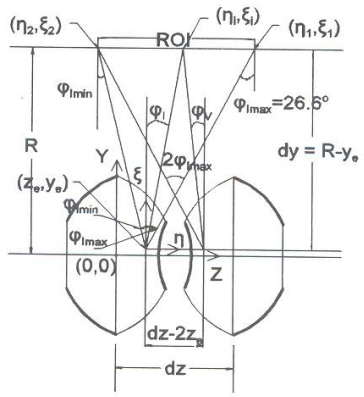

***Figure 4**. Nomenclature for a dual PAL system.*

field angle, φ_I, is measured. The extremes of the ROI are defined by the points

$$(\eta_1, \xi_1) = (dy \tan\varphi_{I_{max}},\ dy)$$
$$= ([R - y_e] \tan\varphi_{I_{max}},\ R - y_e) \quad (3)$$

and

$$(\eta_2, \xi_2) = (dz - 2z_e - dy \tan\varphi_{I_{max}},\ dy)$$
$$= (dz - 2z_e - [R - y_e] \tan\varphi_{I_{max}},\ R - y_e) \quad (4)$$

where φ_{Imax} is equal to 26.6° for the 38 mm (1.5 in.) diameter PAL shown in Fig. 2, (y_e,z_e) is the location of the entrance pupil center of the illuminating PAL measured with respect to an axes system located at its center (0,0), $dy = R-y_e$, dz is the lens spacing measured between the centerlines of the lenses, and R is the radius of the pipe (or the object distance measured perpendicular to the optical axis from the center of the PAL). In these equations, the radius and lens spacing are the only variables present. They depend on the optical setup and the geometry of the object under consideration.

As illustrated in Fig. 4, the location of the point described in Eqn. (3) corresponds to the intersection of the pipe wall with the ray drawn from the entrance pupil center of the illuminating lens at the maximum field angle, φ_{Imax}. The point described in Eqn. (4), on the other hand, corresponds to the intersection of the pipe wall with a ray drawn from the entrance pupil center of the illuminating lens at the minimum field angle associated with the ROI. This field angle is given by

$$\varphi_{I_{min}} = \tan^{-1}\left[\frac{dz - 2z_e - (R - y_e)\tan\varphi_{I_{max}}}{R - y_e}\right] . \quad (5)$$

The length of the ROI is

$$ROI = 2\tan\varphi_{I_{max}}\left(R - y_e - \frac{dz - 2z_e}{2\tan\varphi_{I_{max}}}\right) . \quad (6)$$

The field angle corresponding to the center of the ROI, φ_C, is given by

$$\varphi_{I_C} = \tan^{-1}\left[\frac{(R - y_e)\tan\varphi_{I_{max}} - \frac{ROI}{2}}{R - y_e}\right] \quad (7)$$

where ROI is the length computed from Eqn. (6).

5 PROPAGATION VECTORS

As described in Section 6, the formulation of the phase-displacement equation used for interferometry requires a knowledge of the directions of propagation, γ_i, to and from each point on the test surface under consideration. This knowledge can be obtained by writing Eqn. (2) for the illuminating and viewing lenses as follows:

$$\gamma_I = 1.00417\ \varphi_I - 0.2978 \quad (8)$$

and

$$\gamma_V = 1.00417\ \varphi_V - 0.2978 . \quad (9)$$

It is desirable to express Eqn. (9) in terms of the parameters associated with the illuminating lens. Referring to Fig. 4, the field angle for the viewing lens is

$$\varphi_V = \tan^{-1}\left[\frac{dz - 2z_e - (R - y_e)\tan\varphi_I}{R - y_e}\right] . \quad (10)$$

Since the dual PAL system is symmetrical, Eqn. (10) holds when φ_V and φ_I are interchanged.

By substituting Eqn. (10) into Eqn. (9),

$$\gamma_V = 1.00417\ \tan^{-1}\left[\frac{dz - 2z_e - (R - y_e)\tan\varphi_I}{R - y_e}\right] - 0.2978 . \quad (11)$$

6 INTERFEROMETRIC MEASUREMENTS

The equations developed thus far can be used to quantify measurements made using holo- and/or speckle interferometric techniques.[7-9] In these cases, the linear phase change, δ, that takes place for each point in the ROI is related to the displacement of the point by the well known equation,

$$\delta = n\lambda = (\hat{\mathbf{e}}_I - \hat{\mathbf{e}}_V) \cdot \mathbf{d} = \mathbf{C} \cdot \mathbf{d} \quad (12)$$

where n is the fringe order number and λ is the wavelength. The vectors $\hat{\mathbf{e}}_I$ and $\hat{\mathbf{e}}_V$ are unit vectors in the directions of illumination and observation, respectively; and, $\mathbf{C} = (\hat{\mathbf{e}}_I - \hat{\mathbf{e}}_V)$ is the sensitivity vector along which the displacement vector **d** is projected. The sensitivity vector lies in the plane formed by the illumination and observation vectors, and is directed along their angle bisector.

Referring to Fig. 5, the unit vectors $\hat{\mathbf{e}}_I$ and $\hat{\mathbf{e}}_V$ may be described in terms of the directions of propagation of the illuminating and viewing wavefronts as

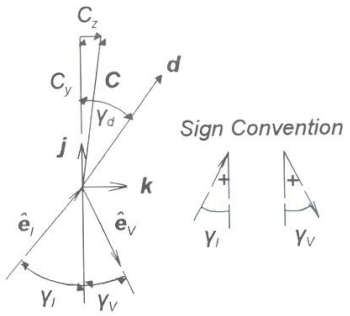

***Figure 5**. The sensitivity vector, **C**, has an out-of-plane (radial) component, C_y, and an in-plane (longitudinal) component, C_z.*

$$\hat{\boldsymbol{e}}_l = \cos\gamma_l\,\boldsymbol{j} + \sin\gamma_l\,\boldsymbol{k} \tag{13}$$

and

$$\hat{\boldsymbol{e}}_V = -\cos\gamma_V\,\boldsymbol{j} + \sin\gamma_V\,\boldsymbol{k} \tag{14}$$

respectively. Thus, the sensitivity vector may be expressed as

$$\begin{aligned}\boldsymbol{C} &= C_y\,\boldsymbol{j} + C_z\,\boldsymbol{k} \\ &= (\cos\gamma_l + \cos\gamma_V)\,\boldsymbol{j} + (\sin\gamma_l - \sin\gamma_V)\,\boldsymbol{k}\end{aligned} \tag{15}$$

The displacement vector can be expressed in terms of its scalar components as

$$\boldsymbol{d} = u\,\boldsymbol{i} + v\,\boldsymbol{j} + w\,\boldsymbol{k} \tag{16}$$

When Eqns. (15) and (16) are substituted into Eqn. (12),

$$\begin{aligned}\delta = n\lambda &= C_y v + C_z w \\ &= (\cos\gamma_l + \cos\gamma_V)\,d\cos\gamma_d \\ &\quad + (\sin\gamma_l - \sin\gamma_V)\,d\sin\gamma_d\end{aligned} \tag{17}$$

where d is the magnitude of the displacement vector and γ_d is the angle that the displacement vector makes with respect to the positive Y axis.

Although the derivation was performed by considering the Y,Z plane, the problem is radially symmetric. Since the terms (d cos γ_d) and (d sin γ_d) represent the out-of-plane (radial) and in-plane (longitudinal) displacement components, respectively, there is no sensitivity to circumferential displacement.

By substituting the propagation vectors defined by Eqns. (8) and (9) into Eqn. (17), the linear phase change is obtained as

$$\begin{aligned}\delta = n\lambda &= [\cos(1.00417\varphi_l - 0.2978) \\ &\quad + \cos(1.00417\varphi_V - 0.2978)]d\cos\gamma_d \\ &\quad + [\sin(1.00417\varphi_l - 0.2978) \\ &\quad + \sin(1.00417\varphi_V - 0.2978)]d\sin\gamma_d\end{aligned} \tag{18}$$

where φ_V is given in terms of φ_l via Eqn. (10). For phase stepping, Eqn. (18) can be written in terms of the angular phase change α, where $\alpha = 2\pi\delta/\lambda$.

A detailed analysis of Eqn. (18) shows that at the center of the ROI, only the radial displacement component is measured. The sensitivity to this component remains nearly constant over the rest of the field. The sensitivity to longitudinal displacement increases linearly with the distance from the center of the ROI.

7 ACKNOWLEDGMENT

Panoramic lenses were secured from Optechnology, Inc., located in Gurley, Alabama.

REFERENCES

[1] **Greguss, P., Gilbert, J.A., Matthys, D.R., Lehner, D.L.,** "Developments in radial metrology," *Proc. of SPIE International Symposium on Optical Engineering and Industrial Sensing for Advanced Manufacturing Technologies*, Vol. 954, Dearborn, Michigan, June 25-30, 1988, pp. 392-398.

[2] **Gilbert, J.A., Leonard, K.M.,** "Experimental mechanics from a different perspective," *Proc. of the 11th. International Conference on Experimental Mechanics*, Oxford, England, August 24-28, 1998; manuscript appears in *Experimental Mechanics - Advances in Design, Testing and Analysis*, edited by I. M. Allison, Balkema Press, 1998, pp. 83-88.

[3] **Fair, S.B.,** "A panoramic electronic speckle pattern interferometer," *Ph.D. Dissertation*, University of Alabama in Huntsville, Huntsville, Alabama, 1998.

[4] **Richter, A.G.,** "Characterization of a panoramic annular lens," *M.S. Thesis*, Marquette University, Milwaukee, WI., 1992.

[5] **Lehner, D.L., Richter, A.G., Matthys, D.R., Gilbert, J.A.,** "Characterization of the panoramic annular lens," *Experimental Mechanics* 36(4): 333-338 (1996).

[6] **Lehner, D.L.,** "Amplitude based radial metrology using panoramic annular lenses," *Ph.D. Dissertation*, University of Alabama in Huntsville, Huntsville, Alabama, 1994.

[7] **Fair, S., Matthys, D.R., Gilbert, J.A.,** "Out-of-plane displacement analysis using panoramic ESPI," *Proc. of the 1999 SEM Spring Conference on Theoretical, Experimental and Computational Mechanics*, Cincinnati, Ohio, June 7-9, 1999, pp. 257-260.

[8] **Lindner, J.L., Gilbert, J.A.,** "A panoramic system for vibration analysis," *Proc. of the SEM IX International Congress on Experimental Mechanics*, June 5-8, 2000.

[9] **Fair, S.B., Gilbert, J.A., Matthys, D.R.,** "Development of a phase-displacement equation for panoramic interferometry," to appear in *Applied Optics*, (2000).